Construction of Shapes Arising from the Minkowski Problem Using a Level Set Approach

Li-Tien Cheng *†

June 15, 2006

Department of Mathematics
University of California, San Diego
9500 Gilman Dr.
La Jolla, CA 92093-0112
phone: (858)534-3894
email: lcheng@math.ucsd.edu

Abstract

The Minkowski problem asks a fundamental question in differential geometry whose answer is not only important in that field but has real world applications as well. We endeavor to construct the shapes that arise from the Minkowski problem by forming a PDE that flows an initial implicitly defined hypersurface to a related configuration under the level set framework. Tools and ideas found in the various applications of level set methods are gathered to generate this PDE. Numerically, its solution is determined by incorporating high order finite difference schemes over the uniform grid available in the framework. Finally, we use our approach in various test cases to generate different shapes arising from different given data in the Minkowski problem.

1 Introduction

Given a compact, strictly convex hypersurface M in $\mathbf{R}^{n+1}$, one can define the Gauss map $G : M \to \mathbf{S}^n$ such that $G(x) \in \mathbf{S}^n$ is in the direction of the

*Deparment of Mathematics, University of California San Diego, La Jolla, California 92093

†Part of this research was completed at Deparment of Mathematics, University of California Los Angeles, Los Angeles, California 90095

unit inward normal at x. This map is in fact a diffeomorphism of M into $\mathbf{S}^n$. Thus, any data on M can be translated to form data on $\mathbf{S}^n$ through the use of the Gauss map. Let K denote the Gauss-Kronecker curvature on M. Then $K \circ G^{-1}$ is a function on $\mathbf{S}^n$ satisfying

$$G_*(d\mu_M) = \frac{1}{K \circ G^{-1}} d\mu_{\mathbf{S}^n},$$

where $d\mu_M$ and $d\mu_{\mathbf{S}^n}$ denote the Lebesgue measures on M and $\mathbf{S}^n$, respectively. Note that if x^i is the ith coordinate function on $\mathbf{S}^n$, then $x^i \circ G$ is a function on M. In fact, for $p \in M$, $x^i \circ G(p)$ is the ith coordinate of the unit normal at p. Therefore,

$$\int_{\mathbf{S}^n} x^i \frac{1}{K \circ G^{-1}} d\mu_{\mathbf{S}^n} = \int_M (x^i \circ G) d\mu_M = 0,$$

which shows that there are some compatibility conditions that a positive function on $\mathbf{S}^n$ has to satisfy in order for it to be the Gauss-Kronecker curvature of a compact, strictly convex hypersurface (ovaloid). The Minkowski problem states that the compatibility condition given above is sufficient for this purpose. In detail,

Minkowski Problem. *Given $F > 0$ on $\mathbf{S}^n$ such that for $i = 1, \ldots, n+1$,*

$$\int_{\mathbf{S}^n} x^i \frac{1}{F} d\mu_{\mathbf{S}^n} = 0,$$

then there exists a compact, strictly convex hypersurface M such that the Gauss-Kronecker curvature at $p \in M$ equals to $F(G(p))$, where $G : M \to \mathbf{S}^n$ is the Gauss map. Moreover, if M' is another solution, then M and M' differ by a translation.

The Minkowski problem is a fundamental problem in differential geometry of roughly a hundred years old that further impacts a fascinating class of elliptic partial differential equations. Its statement was proven in $\mathbf{R}^3$ by Lewy[15] for the real analytic case and Nirenberg[17] for the smooth case, and in general in $\mathbf{R}^{n+1}$ by Cheng and Yau[4] and Pogorelov[23, 24] for the smooth case. We note that in $\mathbf{R}^3$, Gauss-Kronecker curvature of hypersurfaces is called Gauss curvature and is intrinsic. However, in higher dimensions, Gauss-Kronecker curvature does not have this property.

Our interest lies in the inverse problem of constructing M when given F satisfying the compatibility condition. In applications, this is seen, for example, in inverse scattering problems for convex bodies in three dimensional space. More specifically, we find the Minkowski problem appearing in the determination of the shape of a convex body given high frequency

asymptotics of the scattering amplitude from scattering of acoustic or electromagnetic waves off that body. See [16] for more detail and [10, 11] for applications. In addition, the Minkowski problem is found in other areas such as the study of abrasion of metals.

We tackle the construction problem by proposing a PDE based flow on a level set function whose zero level set is the surface of interest. This implicit representation allows for a uniform grid to be placed in $\mathbf{R}^{n+1}$ over which the PDE can be easily discretized using standard high order finite difference schemes. Furthermore, resolution of the surface is automatically handled by this grid. The level set framework also lets us take advantage of an established set of techniques and ideas for the construction and discretization of our evolution PDE (see, e.g., [18]).

Current research in this subject includes the work of [13], which treats the problem as an optimization problem and solves the original polyhedral version of the Minkowski problem following a generalization of Minkowski's proof. More recently the work of [14] considers the Minkowski problem in finite function spaces and is based on Minkowski's isoperimetric inequality. However, as mentioned in [13], the numerical construction of shapes arising from the Minkowski problem has been rather overlooked in general. Among recent theoretical results, we would like to bring attention to [5] which introduces an interesting flow based PDE to the study of the Minkowski problem. We also mention that research exists dealing with inverse problems involving various given curvatures in different frameworks, which is somewhat related to the problem we consider here. Finally, our approach is based on [3].

2 Constructing a Flow

Our first step is to generate a flow that will evolve a surface, as time goes to infinity, to the desired ovaloid arising from the Minkowski problem. Let X denote the surface of interest and let

$$f : X \to \mathbf{R}^{n+1}$$

be the embedding. Furthermore, let ν denote the outward unit normal of the surface and K denote the Gauss-Kronecker curvature. We seek a velocity v, depending on geometric quantities of the surface, in which to evolve f,

$$f_t = v,$$

to achieve our goal. More specifically, we consider only flow in the inward normal direction,

$$f_t = -v_n \nu,$$

since the tangential part of flow velocity does not more the actual surface, only changing parametrization. The desired v_n should have the property that $v_n = 0$ when the surface forms the desired ovaloid. This means the desired ovaloid is a steady state solution of the flow, a property needed to obtain convergence. Furthermore, we would like the evolution PDE to be of at most second order to avoid the difficulties of higher order PDE's. We of course expect at least second order due to the probable use of Gauss-Kronecker curvature in the flow.

The desired ovaloid can be identified through the property

$$K = F(-\nu),$$

which is equivalent to $K = F \circ G$ seen in the statement of the Minkowski problem. Thus, a valid v_n will equal zero for an ovaloid satisfying $K = F(-\nu)$. However, simple guesses based on this property fail to produce adequate flows, resulting either in backward parabolic PDE's or the desired ovaloid forming an unstable equilibrium. For example, the choice

$$v_n = K - F(-\nu)$$

satisfies the property that $v_n = 0$ if and only if the surface is the desired ovaloid. However, suppose $F \equiv 1$, which means the desired ovaloid is the sphere of radius 1. Furthermore, suppose the current surface is a sphere of radius greater than 1. Then the Gauss-Kronecker curvature of this surface is a constant less than 1. Thus v_n will be negative, implying that the sphere will expand and hence move away from the unit sphere. Similarly, a sphere of radius less than 1 will shrink, also moving away. Thus the flow using this choice of v_n will not generate the correct ovaloid. Also, the proposed fix of letting $v_n = F(-\nu) - K$ produces a backward parabolic evolution equation. Other simple choices of v_n such as $v_n = \pm\left(\frac{K}{F(-\nu)} - 1\right)$ or $v_n = \pm\frac{1}{F - K}$ encounter the same difficulties. Thus constructing a flow that will give convergence to an ovaloid satisfying $K = F(-\nu)$ may not be an easy task.

We may, however, change the problem to achieve a slightly different and more manageable goal. We look instead at flow in the inward normal direction by speed $\frac{K}{F(-\nu)}$ but under a preserved enclosed volume constraint. Thus we set

$$v_n = \frac{K}{F(-\nu)} - \lambda,$$

where λ is a constant depending on time chosen to preserve the enclosed volume of the surface. This techinque is usually seen in variational problems,

where λ serves as a Lagrange multiplier. For example, in the construction of Wulff crystal shapes, which are compact, strictly convex surfaces, the Wulff surface energy is minimized with a given enclosed volume constraint. Minimization can be achieved through gradient descent to steady state on the energy and constraint, leading to a PDE based flow (see, e.g., [19]). The same enclosed volume constraint can also be found in the study of soap bubbles, in structural engineering, and in geometrically based motions[12, 18].

Note, however, that the introduction of the volume constraint to our flow means that steady state solutions are no longer required to be the desired ovaloids arising from the Minkowksi problem. In fact, if the evolved surface reaches steady state, it will satisfy $v_n = 0$, which translates to

$$K = \lambda_\infty F(-\nu),$$

where λ_∞ is some constant. This means that though the Gauss-Kronecker curvature of the final surface will no longer equal, in general, to the prescribed values, the final surface will just be a dilation of the desired ovaloid. Thus our new flow seeks a dilated solution to our original problem. It may be more advantageous to have the dilated solution than the real solution due to resolution issues that appear under the numerical discretization. However, we can always recover the real solution from the actual one through the value of λ_∞. In fact, a dilation of $\left(\frac{1}{\lambda_\infty}\right)^{\frac{1}{n}}$ will return the surface to the desired ovaloid arising from the Minkowski problem.

3 Level Set Representation of Hypersurfaces

We now seek the expressions of the quantities ν, K, and λ in terms of f and its derivatives. More accurately, we will represent the surface implicitly and derive the desired quantities, as well as the form of the evolution PDE, in this setting. We use the level set framework[20] as our implicit framework. Here, the surface is replaced by a real valued function defined over $\mathbf{R}^{n+1}$ whose zero level set is the surface. Such a function is called a level set function and usually denoted by ϕ. Thus in the level set framework, we replace all mention of the surface by the level set function ϕ. The advantage of considering ϕ in place of just its zero level set surface is in the numerical algorithm we construct and consider later. We refer the basics of level set methods to [18].

Various geometric quantities of the surface such as mean curvature and surface area can all be written in terms of ϕ, however, we are interested here

specifically in the expressions for ν, K, and λ. For definiteness, let the set of points satisfying $\phi < C$ denote the inside of the C level set surface of ϕ and $\phi > C$ denote the outside. Then the outward normal vector of that surface at any point equals

$$\nu = \frac{\nabla\phi}{|\nabla\phi|}.$$

Thus, when viewed on the zero level set surface of ϕ, $-\nu$ forms the expression for the inward normals of the surface of interest. The Gauss-Kronecker curvature on the other hand can be obtained from the level set representation of the second fundamental form,

$$\frac{1}{|\nabla\phi|} P_{\nabla\phi} \nabla^2 \phi P_{\nabla\phi},$$

where P_v denotes the orthogonal projection matrix that projects vectors onto the plane with normal vector v (see, e.g., [2]). This matrix form of the second fundamental form is symmetric and has one zero eigenvalue, with associated eigenvector $\nabla\phi$. The product of the other eigenvalues, called the principle eigenvalues, gives the Gauss-Kronecker curvature K. This means that this product evaluated at a point on the C level set surface of ϕ gives the Gauss-Kronecker curvature of that surface at that point. We are of course especially interested in K on the zero level set surface of ϕ. Specifically, for $n = 2$, we can explicitly derive the formulas for the two principle curvatures. Let a_{ij}, $i, j = 1, 2, 3$ denote the terms in the matrix of the second fundamental form. Then the roots of the cubic characteristic polynomial $p(\sigma) = \det(a_{ij} - \sigma\delta_{ij})$, where δ_{ij} denotes the Kronecker delta, give the eigenvalues of the matrix. We note that the coefficient of the σ to the power zero term of p must be zero as $\sigma = 0$ is a root of the polynomial. Thus we are interested in the roots of the quadratic polynomial $\frac{p(\sigma)}{\sigma}$. This polynomial takes the form

$$-\sigma^2 + (a_{11} + a_{22} + a_{33})\sigma + (a_{12}^2 - a_{11}a_{22}) + (a_{13}^2 - a_{11}a_{33}) + (a_{23}^2 - a_{22}a_{33}).$$

The product of its roots, coming from the quadratic formula, can thus be written as

$$(a_{11}a_{22} - a_{12}^2) + (a_{11}a_{33} - a_{13}^2) + (a_{22}a_{33} - a_{23}^2).$$

When a_{ij}, $i, j = 1, 2, 3$ is written in terms of ϕ, we get the desired form of Gauss curvature in the level set framework. We will deal with the expression for λ after we consider the evolution equation in terms of ϕ. Surface area and enclosed volume of level set surfaces will also come up at that time.

For evolution in the level set framework, given a velocity field v defined in $\mathbf{R}^{n+1}$, motion of the level set surfaces of ϕ under v is obtained through the transport equation

$$\phi_t + v \cdot \nabla\phi = 0.$$

In order to handle more general motions, we can let v depend on ϕ and its derivatives. We are interested here especially in the case

$$v = -v_n \frac{\nabla\phi}{|\nabla\phi|},$$

which gives motion of level set surfaces in the inward normal direction by speed v_n defined in $\mathbf{R}^{n+1}$. The equation thus takes the form

$$\phi_t = v_n |\nabla\phi|.$$

The inward normal motion we wish to use was defined previously only on the surface of interest. This motion needs to be extended to a flow for all the level set surfaces of ϕ in order to be used in the above level set evolution equation. For example, the velocity can be computed first on the surface and then extended off the surface to $\mathbf{R}^{n+1}$ constant in the normal directions. Numerically, this can be handled by fast marching[8, 26, 31] or fast sweeping methods[6, 30]. However, for our problem, we may simply assign the same type of motion, except the volume constraint part, to the other level set surfaces of ϕ. Thus we let

$$v_n = \frac{K}{F(-\nu)} - \lambda,$$

where λ is a constant function of time that is chosen to preserve only the volume of the zero level set during the flow. Under this flow, each level set surface moves under its own Gauss-Kronecker curvature and related to its own normals but also with repect to λ chosen specifically from the zero level set. Thus the form of the evolution equation we use for ϕ is

$$\phi_t = \left(\frac{K}{F(-\nu)} - \lambda \right) |\nabla\phi|.$$

Note, this flow makes the most sense at the zero level set of ϕ and we are in fact interested not necessarily in the convergence of the whole level set function, but just in the zero level set. If the zero level set surface reaches steady state, it will satisfy $K = \lambda_\infty F(-\nu)$ and will thus be a desired dilated solution. To complete the level set evolution equation, we just need to determine λ from ϕ and its derivatives.

The expression for λ, following the procedure of [25], can be generated from its role in fixing the volume enclosed by the zero level set surface in time. The volume itself takes the form

$$\int_{\mathbf{R}^{n+1}} H(-\phi)\ dx,$$

where H denotes the one dimensional Heaviside function. Thus λ can be chosen to satisfy

$$\frac{d}{dt}\int_{\mathbf{R}^{n+1}} H(-\phi)\ dx = 0.$$

Inputting the evolution equation into this and simplifying leads to

$$\begin{aligned}
0 &= \frac{d}{dt}\int_{\mathbf{R}^{n+1}} H(-\phi)\ dx \\
&= \int_{\mathbf{R}^{n+1}} \delta(\phi)\phi_t\ dx \\
&= \int_{\mathbf{R}^{n+1}} \delta(\phi)v_n|\nabla\phi|\ dx \\
&= \int_{\mathbf{R}^{n+1}} \delta(\phi)\left(\frac{K}{F(-\nu)} - \lambda\right)|\nabla\phi|\ dx \\
&= \int_{\mathbf{R}^{n+1}} \delta(\phi)\frac{K}{F(-\nu)}|\nabla\phi|\ dx - \int_{\mathbf{R}^{n+1}} \delta(\phi)\lambda|\nabla\phi|\ dx,
\end{aligned}$$

where δ denotes the one dimensional delta function. Thus solving for λ from this, we obtain

$$\lambda = \frac{\displaystyle\int_{\mathbf{R}^{n+1}} \delta(\phi)\frac{K}{F(-\nu)}|\nabla\phi|\ dx}{\displaystyle\int_{\mathbf{R}^{n+1}} \delta(\phi)|\nabla\phi|\ dx}.$$

The numerator is the integral of the quantity $\frac{K}{F(-\nu)}$ over the zero level set surface and the denominator is the area of that surface. Thus λ is the average of $\frac{K}{F(-\nu)}$ over the zero level set surface. This gives the final piece of the level set evolution equation. We would like to note here that other evolution equations may also give the properties we want, such as

$$\phi_t = (K - \lambda F(-\nu))|\nabla\phi|,$$

where λ once again preserves enclosed volume during the flow. These may even have advantages over our chosen PDE, however, this needs to be determined through further studies and so we stick with the form we have derived previously.

We would like to mention that we do not yet have theoretical justification that our flow converges starting with an initial ovaloid. In fact, we assume, though we have no proof, that the flow preserves smoothness and strict convexity of the evolving surface. The convexity issue is important since the evolution PDE, which involves Gauss-Kronecker curvature, is not parabolic for surfaces that are not strictly convex. We hope the various missing information will be completed in the future, however, at the moment we rely purely on justifications through numerical simulations.

4 Numerical Solution of the Evolution Equation

In our level set framework, we work in the ambient space $\mathbf{R}^{n+1}$ on the level set function rather than directly on the surface of interest. Thus, numerically, we may lay down a uniform grid over $\mathbf{R}^{n+1}$, or more precisely in some finite domain of $\mathbf{R}^{n+1}$, and work over this grid. Operating over a static, uniform grid rather than a dynamic, irregular one parametrizing the surface allows us to use standard, well studied high order finite difference schemes to discretize the various geometric quantities we have as well as the evolution PDE in general. Furthermore, a grid set on the surface may not preserve uniform resolution of the surface at later time. Interpolation and reparmetrization must be used to regrid the surface or add points at places where there are not enough. The uniform grid of the level set framework, on the other hand, will automatically resolve the surfaces of interest throughout the flow. Thus the level set framework greatly simplifies the numerical considerations of the problem and allows us to easily and accurately construct the desired dilated ovaloids of the Minkowski problem.

In our implementation, we choose the finite domain $[-1,1] \times [-1,1] \times [-1,1]$ to operate in. The evolution PDE takes the form

$$\phi_t = \frac{K}{F(-\nu)}|\nabla\phi| - \lambda|\nabla\phi|.$$

For this, we use second order central differencing over the uniform grid to discretize the spatial derivatives of ϕ found in the expressions of K, ν, and λ as well as the $|\nabla\phi|$ of the first term on the right hand side of the equation. In the expression of λ, the delta function is replaced by a smoothed out delta function, with width around $6\Delta x$. Thus the integral can be easily approximated to second order accuracy as the integrand is zero only at gridpoints close to the zero level set. We simply add together the value of the integrand at each grid point multiplied by the volume of the each

gridcube, $\Delta x \cdot \Delta y \cdot \Delta z$, for this. Finally, the $|\nabla\phi|$ term multiplying λ in the evolution equation is of Hamilton-Jacobi form and we discretize it using fifth order WENO-Godunov[9]. Other choices for this include third order ENO-Godunov[21] or lower order ENO or WENO schemes. For the time derivative on ϕ, we use Forward Euler, though Runge-Kutta schemes such as third order TVD-RK[27] or fourth order SSP-RK[28] can be used in its place. Accuracy studies of this discretization will be presented later in test cases. Finally, we note that there may be certain points where the denominators of the expressions for K and ν are zero. We remove these singularities by adding a small number ϵ to their denominators and extending F to be homogeneous of degree zero off $\mathbf{S}^n$ into $\mathbf{R}^{n+1}$.

We can start this algorithm simply with an initial ϕ with zero level set forming a sphere in our finite domain at time zero. Of course, an initial guess that is closer to the final solution would give faster convergence but a sphere is adequate when no such additional analysis or information is available. The algorithm can then be run until the zero level set converges. Note an advantage of searching for the dilated ovaloid of the Minkowski problem rather than the actual one is that the dilated ovaloid is usually of a manageable size, due to the constraint on the volume. This property helps keep the flowing surface of interest within the finite domain and also helps resolve the surface. On the other hand, without additional analysis or information, a surface attempting to flow to the actual ovaloid may exit the finite domain or attain a size smaller than the underlying grid can resolve. To determine convergence of the zero level set of the level set function, we have several choices for stopping conditions. One of them consists of considering the volume of the difference,

$$\int_{\mathbf{R}^{n+1}} |H(\phi_1) - H(\phi_2)| \, dx,$$

of the zero level sets of the level set function at two different times. Here, ϕ_1 and ϕ_2 denote the level set function ϕ at those two times. If this difference is smaller than a given tolerance, then the algorithm can be stopped and convergence can be assumed. On the other hand, the location of the zero level sets of ϕ_1 and ϕ_2 can be found and the maximum distance between these sets of points can be used as the criterion. Finally, the magnitude of $\left|\frac{K}{F(-\nu)} - \lambda\right|$ on the zero levels set surface can be used instead. Once convergence is achieved and the algorithm is stopped, we can plot the final shape by recovering the zero level set of the level set function through interpolation. Standard algorithms for this exist and, for example, can be found

in Matlab's collection of functions. This completes the algorithm coming from our previous analysis of the problem, from initial condition to numerical flow to final shape and the recovery of it. However, further numerical considerations need to be addressed that will modify it.

5 Further Numerical Considerations

One important consideration is the need for better forms of level set functions as opposed to arbitrary ones. This is to prevent the level set function from becoming too steep or flat near its zero level set, thus reducing the accuracy of our discretization schemes. Furthermore, accuracy in obtaining the location of the zero level set surface for plotting purposes can also be seriously affected. Note in our application, if we are given $F \equiv 1$ and $\phi = |x| - r$ at a certain time, then the zero level set of ϕ, which already forms the desired solution, does not move under the evolution equation. Also, K is a constant for each level set surface of ϕ. In fact, for positive level sets, this constant is less than the constant associated with the zero level set and vice versa for negative level sets. However, the λ used is the same for all the level sets. Therefore, the positive level sets expand and the negative level sets shrink under the flow. This makes ϕ flat near its zero level set. Furthermore, we expect this phenomenon not only in this example, but in general. One solution to this problem is to enforce that the level set function is a signed distance function, where the value of the function at a point is the distance of that point away from the zero level set surface, with a negative sign if the point is on the inside of that surface. This form is commonly used in level set applications and can be enforced by solving to steady state a specific PDE, called the reinitialization PDE, at each time step (see, e.g., [22, 29]). Alternatively, fast marching or fast sweeping methods can be used. In our implementation, the reinitialization PDE at each time step is solved to obtain the signed distance function. We do note that this may not be the best form to use since the level set function will generally not be smooth everywhere, however, it seems to be adequate in our simulations. Also, note the level set surfaces of the signed distance function will be compact and strictly convex if the zero level set surface is so. This is important for the parabolicity of the evolution PDE for the level set function. In fact, if convexity is of concern during the flow, since we have no proof that it is preserved, the value for K can be set to zero at points, if they exist, where the minimal principal curvature, i.e., the smallest eigenvalue of the second fundamental form matrix, is negative.

Enforcing signed distance functions at each time step also plays a role in efficiency. Instead of operating in $[-1,1] \times [-1,1] \times [-1,1]$, we may just consider gridpoints in a neighborhood of the zero level set surface, with the size of the neighborhood directly related to the size of the stencils of the difference schemes used on the evolution PDE. This greatly reduces the number of computations needed in the algorithm, as well as alleviating memory requirements, and transforms the algorithm to what is known as a local level set method (see [1, 22]). Also, we note that working in the neighborhood allows us to largely ignore the points where K and ν have zero denominators as these points usually lie far from the zero level set surface. The use of signed distance functions is in creating the neighborhood of interest, which can simply be the gridpoints of a certain distance away from the zero level set surface. This distance, when taken to be a constant multiplied by the grid stepsize, allows our algorithm to be roughly equivalent in optimality to operating directly on the surface of interest. Furthermore, the enforcing of signed distance on the level set function will remove any negative effects that the boundary of the neighborhood may introduce at each time step in our finite difference schemes. Finally, we note that we do not actually need very accurate values for signed distance, nor do we need signed distance everywhere but just at a few gridpoints away from the zero level set surface. Thus the reinitialization PDE does not really need to be solved to steady state in practice but only iterated a few times. In our implementation, we follow [22] and discretize the reinitialization PDE, which is of Hamilton-Jacobi form, using TVD-RK of third order in time and WENO-Godunov of fifth order in space. Furthermore, we iterate this PDE only twice per time step and this seems to be adequate in our simulations.

Another important modification involves volume preservation. In test simulations of our algorithm, we noticed that though we attempt to enforce a preservation of volume through our introduction of λ, there is actually an accumulation of volume loss that may, on occasion, become considerable and is at least annoying. This, we believe, is due to our trying to set the change in volume to zero. Because of approximations in the numerical scheme, however, this change is not exactly zero at each time step and this error may lead to an accumulating loss of volume. In other words, there is no mention, in our algorithm, of the volume of the original ovaloid and so there can be no safeguard for returning the volume of the evolving surface to the original volume when the difference becomes great. This leads us to calculate the volume enclosed by the evolving surface at each time step and compare it to the volume of the original ovaloid. With this added information, we

modify the value given to

$$\frac{d}{dt}\int_{\mathbf{R}^{n+1}} H(-\phi)\ dx,$$

not setting it equal to zero, but to the divided difference involving the volume of the current surface and that of the surface at the previous time step. We furthermore replace the latter quantity by assuming the previous surface encloses a volume equal to that of the original surface. Thus, the expression for λ becomes

$$\lambda = \frac{\displaystyle\int_{\mathbf{R}^{n+1}} \delta(\phi)\frac{K}{F(-\nu)}|\nabla\phi|\ dx - \frac{1}{\Delta t}\left(\int_{\mathbf{R}^{n+1}} H(-\phi)\ dx - \int_{\mathbf{R}^{n+1}} H(-\phi_0)\ dx\right)}{\displaystyle\int_{\mathbf{R}^{n+1}} \delta(\phi)|\nabla\phi|\ dx},$$

where ϕ_0 denotes the initial level set function. The volumes in this expression can be approximated over the grid by using a standard quadrature rule and a smoothed out Heaviside function. We do note that calculation of volume affects the efficiency of the algorithm since not all operations are performed local to the zero level set surface. However, there may be techniques to save the efficiency since only the number of gridpoints away from the zero level set and enclosed by the surface needs to be calculated as a part of determining the volume. Regardless of this, the local level set method still speeds up the original global approach and furthermore reduces the memory required. Altogether, these changes give our final algorithm for constructing dilated shapes arising from the Minkowski problem.

6 Results on Different Test Cases

The derivation of our algorithm applies for general n, however, for n large, grid based methods become prohibitively expensive. We concentrate on the physically relevant case of $n = 2$, i.e., surfaces in $\mathbf{R}^3$. In our simulations, we do not actually dilate the final surfaces from our evolution PDEs to recover the correct one arising from the Minkowski problem since the dilated surfaces already have the correct basic shape and furthermore possess a more manageable size. We begin our tests on ellipsoids, since they have easily computable expressions for Gauss curvature (see, e.g., [7]). Using these expressions for F, we can test our algorithm on different ellipsoids. For our simulations, we mostly use a $50 \times 50 \times 50$ grid. Figure 1 and 2 show our results on two ellipsoids with different axes lengths. Table 1 shows that our algorithm applied to the ellipsoid of Figure refellip1 seems to be

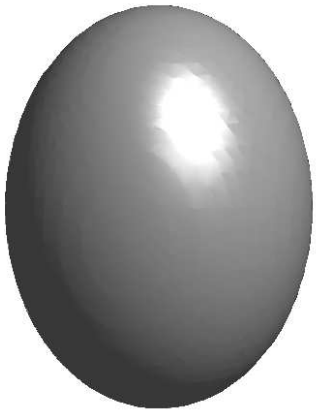

Figure 1: An ellipsoid generated using our algorithm. This example was used for accuracy analysis in Table 1

second order accurate and also that the volume is well preserved, with the final volume close to the original one. Here the approximate solution was compared directly to the exact one.

We also tested our algorithm on other types of ovaloids. In fact, a simple way to create F to ensure that the compatibility condition of the Minkowski problem is satisfied is to enforce enough symmetry in F, for example, $F(x, y, z) = F(-x, y, z) = F(x, -y, z) = F(x, y, -z)$ for $x^2 + y^2 + z^2 = 1$. This simplification still leads to a variety of interesting shapes. Figure 3 shows the results of an F generating a slightly smoothed out surface composed of two spherical caps glued together. The smoothing is to ensure

grid size	error	order	volume change
$25 \times 25 \times 25$	0.0050		$3.61355 \cdot 10^{-5}$
$50 \times 50 \times 50$	0.0014	1.8797	$2.02033 \cdot 10^{-6}$
$100 \times 100 \times 100$	$3.1342 \cdot 10^{-4}$	2.1163	$2.84314 \cdot 10^{-7}$

Table 1: Order of accuracy and volume change analysis when the solution is an ellipsoid.

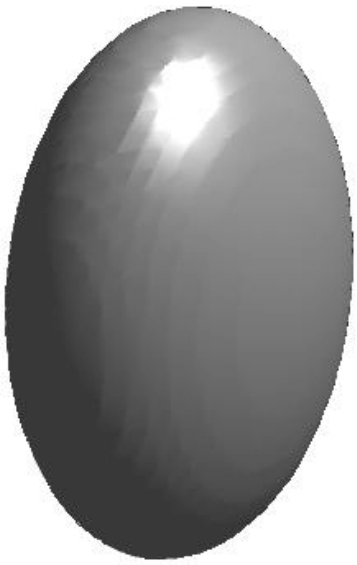

Figure 2: Another ellipsoid with different axes lengths generated using our algorithm.

F is bounded, however, note that the edge where gluing has occurred is still relatively sharp. Figure 4 shows the results of an F arising from a slightly smoothed out surface composed of two conical caps glued together. The smoothing in this case not only bounds F but enforces strict convexity. Nevertheless, the figure still displays rather sharp corners and edges and rather flat side profiles. Figure 5 shows the results of an F approximating a heavily smoothed out cylinder. In this case, the edges are not sharp due to our choice of F but the sides still retain some degree of flatness. This is also the case for Figure 6, where the shape is a heavily smoothed out multifaceted surface.

Finally, we consider more general tests where F does not satisfy all the symmetry conditions of the previous examples. Figure 7 shows the results of an F representing a surface composed of a sphere glued together with an ellipse. Finally, Figure 8 shows the results of an F from a smoothed out version of a sphere glued together with a cone. We are able to recover the shapes in both cases.

In each test case, our the evolving surface under our algorithm converged either to the exact dilated solution, when it can be derived, or to what we believe to be the exact one, sharing all the characteristics of the desired

Figure 3: A smoothed out surface of two spherical caps generated using our algorithm.

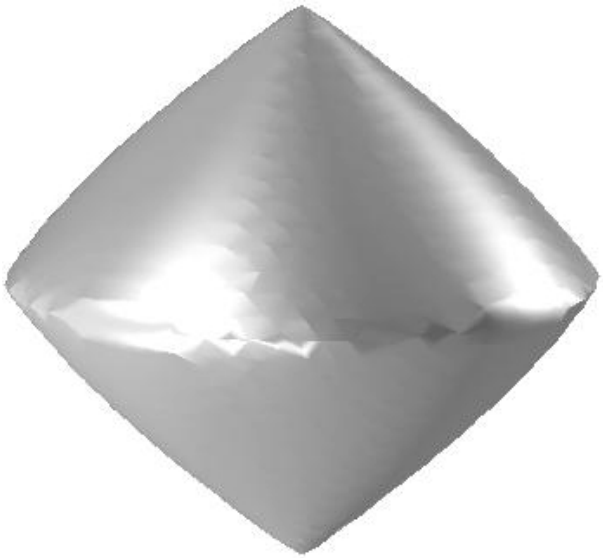

Figure 4: A smoothed out surface of two conical caps generated using our algorithm.

Figure 5: A smoothed out cylinder generated using our algorithm.

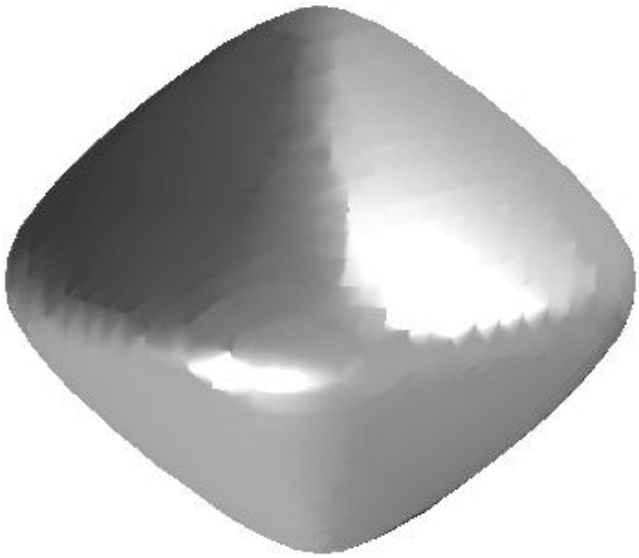

Figure 6: A smoothed out multifaceted surface generated using our algorithm.

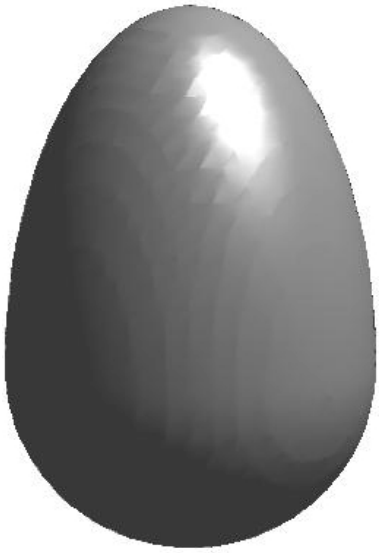

Figure 7: An surface consisting of a sphere glued to an ellipse generated using our algorithm.

Figure 8: An surface consisting of a sphere glued to a cone generated using our algorithm.

ovaloid. In fact, the results show that our approach can handle near degenerate cases of given F. Furthermore, the volume changes are negligible for the flowing surfaces, the final shapes are well resolved and of manageable size, and convexity seems to be preserved during evolution in each case. These numerical studies hint that the evolution PDE and algorithm we have constructed can be proven to be valid.

7 Conclusion

We have introduced an evolution PDE that constructs dilated versions of ovaloids arising from the Minkowski problem. Using the level set framework, our algorithm based on the flow can take advantage of a uniform grid in the ambient space. Thus well resolved, accurate solutions can be obtained. Furthermore, ideas and techniques found in level set methods, such as the local level set method for efficiency, can be brought to bear. In simulations, we observe our algorithm satisfying several desired properties such as preservation of volume and convexity, but most importantly convergence. Finally, the dilated solutions, though themselves possessing advantageous characteristics, can be easily transformed to recover the actual ovaloids of the Minkowski problem. Thus we have introduced a simple geometric flow based level set approach to constructing shapes arising from the Minkowski problem.

8 Acknowledgments

The author would like to thank Hsiao-Bing Cheng, Shiu-Yuen Cheng, and Kai Hu for helpful discussions in differential geometry and Stanley Osher for suggestions in the numerical aspects of the problem. The author would further like to thank Shiu-Yuen Cheng for introducing the author to the Minkowski problem and the possibility of a numerical solution.

References

[1] D. Adalsteinsson and J.A. Sethian. A Fast Level Set Method for Propagating Interfaces. *J. Comput. Phys.*, 118:269–277, 1995.

[2] L. Ambrosio and H.M. Soner. Level Set Approach to Mean Curvature Flow in Arbitrary Codimension. *Journal of Differential Geometry*, 43:693–737, 1996.

[3] L.-T. Cheng. *The Level Set Method Applied to Geometrically Based Motion, Materials Science, and Image Processing*. PhD thesis, Univeristy of California, Los Angeles, 2000.

[4] S.Y. Cheng and S.T. Yau. On the Regularity of the Solution of the n-dimensional Minkowski Problem. *Comm. Pure Appl. Math.*, 29:495–516, 1976.

[5] K.-S. Chou and X.-J. Wang. A Logarithmic Gauss Curvature Flow and the Minkowski Problem. *Ann. Inst. H. Poincaré Anal. Non Lineaire*, 17(6):733–751, 2000.

[6] P. Danielsson. Euclidean Distance Mapping. *Computer Graphics and Image Processing*, 14:227–248, 1980.

[7] M. do Carmo. *Differential Geometry of Curves and Surfaces*. Prentice-Hall, Inc., 1976. Translated from the Portuguese.

[8] J. Helmsen, E. Puckett, P. Colella, and M. Dorr. Two New Methods for Simulating Photolithography Development in 3D. *Proc. SPIE*, 2726:253–261, 1996.

[9] G.S. Jiang and D. Peng. Weighted ENO Schemes for Hamilton Jacobi Equations. *SIAM J. Scient. Comput.*, 21(6):2126–2143, 2000.

[10] M. Kaasalainen, L. Lamberg, and K. Lumme. Interpretation of Lightcurves of Atmosphereless Bodies. 2. Practical Aspects of Inversion. *Astron. Astrophys.*, 259:333–340, 1992.

[11] M. Kaasalainen, L. Lamberg, K. Lumme, and E. Bowell. Interpretation of Lightcurves of Atmosphereless Bodies. 1. General Theory and New Inversion Schemes. *Astron. Astrophys.*, 259:318–332, 1992.

[12] M. Kang, B. Merriman, S. Osher, and P. Smereka. Level Set Approach for the Motion of Soap Bubbles with Curvature Dependent Velocity or Acceleration. CAM Report 96-19, UCLA, 1996.

[13] L. Lamberg. *On the Minkowski Problem and the Lightcurve Operator*. PhD thesis, Univeristy of Helsinki, 1993.

[14] L. Lamberg and M. Kaasalainen. Numerical Solution of the Minkowski Problem. *J. of Comput. Appl. Math.*, 137(2):213–227, 2001.

[15] H. Lewy. On Differential Geometry in the Large 1 (Minkowski's Problem). *Trans. Amer. Math. Soc.*, 43(2):258–270, 1938.

[16] A. Majda. The Inverse Problem for Convex Bodies. *Proc. Natl. Acad. Sci. USA*, 73(5):1377–1378, 1976.

[17] L. Nirenberg. The Weyl and Minkowski Problems in Differential Geometry in the Large. *Commun. Pure Appl. Math.*, 6:337–394, 1953.

[18] S. Osher and R. Fedkiw. Level Set Methods: An Overview and Some Recent Results. *J. Comput. Phys.*, 169:463–502, 2001.

[19] S. Osher and B. Merriman. The Wulff Shape as the Asymptotic Limit of a Growing Crystal Interface. *Asian J. Math.*, 1(3):560–571, 1997.

[20] S. Osher and J.A. Sethian. Fronts Propagating with Curvature Dependent Speed: Algorithms Based on Hamilton-Jacobi Formulations. *J. Comput. Phys.*, 169(1):12–49, 1988.

[21] S. Osher and C.-W. Shu. High order essentially non-oscillatory schemes for Hamilton-Jacobi equations. *SINUM*, 28:907–922, 1991.

[22] D. Peng, B. Merriman, S. Osher, H. Zhao, and M. Kang. A PDE-Based Fast Local Level Set Method. *J. Comput. Phys.*, 155(2):410–438, 1999.

[23] A.V. Pogorelov. The Multidimensional Minkowski Problem. *Izdat. "Nauka", Moscow*, 1975.

[24] A.V. Pogorelov. *The Multidimensional Minkowski Problem*. J. Wiley, 1978.

[25] L. Rudin, S. Osher, and E. Fatemi. Nonlinear Total Variation Based Noise Removal Algorithms. *Physica D*, 60:259–268, 1992.

[26] J.A. Sethian. Fast Marching Level Set Methods for Three Dimensional Photolithography Development. *Proc. SPIE*, 2726:261–272, 1996.

[27] C.-W. Shu and S. Osher. Efficient Implementation of Essentially Nonoscillatory Shock-Capturing Schemes. *J. Comput. Phys.*, 77(2):439–471, 1988.

[28] R.J. Spiteri and S.J. Ruuth. A New Class of Optimal High-Order Strong-Stability-Preserving Time Discretization Methods. To appear in SINUM.

[29] M. Sussman, P. Smereka, and S. Osher. A Level Set Method for Computing Solutions to Incompressible Two-Phase Flow. *J. Comput. Phys.*, 114:146–159, 1994.

[30] Y.-H. Tsai, L.-T. Cheng, S. Osher, and H.K. Zhao. Fast Sweeping Algorithms for a Class of Hamilton-Jacobi Equations. CAM Report 01-27, UCLA, 2001. Submitted to SINUM.

[31] J.N. Tsitsiklis. Efficient Algorithms for Globally Optimal Trajectories. *IEEE Transactions on Automatic Control*, 50:1528–1538, 1995.